Furosemide as a possible therapeutic for COVID-19 (#47843)

First submission

Guidance from your Editor

Please submit by 3 May 2020 for the benefit of the authors (and your \$200 publishing discount).



Structure and Criteria

Please read the 'Structure and Criteria' page for general guidance.



Custom checks

Make sure you include the custom checks shown below, in your review.



Raw data check

Review the raw data.



Image check

Check that figures and images have not been inappropriately manipulated.

Privacy reminder: If uploading an annotated PDF, remove identifiable information to remain anonymous.

Files

Download and review all files from the <u>materials page</u>.

18 Figure file(s)

3 Table file(s)

1 Raw data file(s)



Cell line checks



Is the correct provenance of the cell line described?

Structure and Criteria



Structure your review

The review form is divided into 5 sections. Please consider these when composing your review:

- 1. BASIC REPORTING
- 2. EXPERIMENTAL DESIGN
- 3. VALIDITY OF THE FINDINGS
- 4. General comments
- 5. Confidential notes to the editor
- Prou can also annotate this PDF and upload it as part of your review

When ready <u>submit online</u>.

Editorial Criteria

Use these criteria points to structure your review. The full detailed editorial criteria is on your guidance page.

BASIC REPORTING

- Clear, unambiguous, professional English language used throughout.
- Intro & background to show context.
 Literature well referenced & relevant.
- Structure conforms to <u>PeerJ standards</u>, discipline norm, or improved for clarity.
- Figures are relevant, high quality, well labelled & described.
- Raw data supplied (see <u>PeerJ policy</u>).

EXPERIMENTAL DESIGN

- Original primary research within Scope of the journal.
- Research question well defined, relevant & meaningful. It is stated how the research fills an identified knowledge gap.
- Rigorous investigation performed to a high technical & ethical standard.
- Methods described with sufficient detail & information to replicate.

VALIDITY OF THE FINDINGS

- Impact and novelty not assessed.
 Negative/inconclusive results accepted.
 Meaningful replication encouraged where rationale & benefit to literature is clearly stated.
- All underlying data have been provided; they are robust, statistically sound, & controlled.
- Speculation is welcome, but should be identified as such.
- Conclusions are well stated, linked to original research question & limited to supporting results.

Standout reviewing tips



The best reviewers use these techniques

Τ	p

Support criticisms with evidence from the text or from other sources

Give specific suggestions on how to improve the manuscript

Comment on language and grammar issues

Organize by importance of the issues, and number your points

Please provide constructive criticism, and avoid personal opinions

Comment on strengths (as well as weaknesses) of the manuscript

Example

Smith et al (J of Methodology, 2005, V3, pp 123) have shown that the analysis you use in Lines 241-250 is not the most appropriate for this situation. Please explain why you used this method.

Your introduction needs more detail. I suggest that you improve the description at lines 57-86 to provide more justification for your study (specifically, you should expand upon the knowledge gap being filled).

The English language should be improved to ensure that an international audience can clearly understand your text. Some examples where the language could be improved include lines 23, 77, 121, 128 - the current phrasing makes comprehension difficult.

- 1. Your most important issue
- 2. The next most important item
- 3. ...
- 4. The least important points

I thank you for providing the raw data, however your supplemental files need more descriptive metadata identifiers to be useful to future readers. Although your results are compelling, the data analysis should be improved in the following ways: AA, BB, CC

I commend the authors for their extensive data set, compiled over many years of detailed fieldwork. In addition, the manuscript is clearly written in professional, unambiguous language. If there is a weakness, it is in the statistical analysis (as I have noted above) which should be improved upon before Acceptance.



Furosemide as a possible therapeutic for COVID-19

Zhiyu Wang ^{1, 2}, Yanfei Wang ¹, Prachi Vilekar ¹, Seung-Pil Yang ¹, Mayuri Gupta ¹, Myong In Oh ¹, Autumn Meek ¹, Lisa Doyle ¹, Anja Brennecke ¹, Imindu Liyanage ^{1, 3}, Mark Reed ¹, Christopher Barden ¹, Donald F Weaver ^{Corresp. 1, 2, 3}

Corresponding Author: Donald F Weaver Email address: dweaver@uhnres.utoronto.ca

The novel coronavirus SARS-CoV-2 has become a global health concern. The morbidity and mortality of the potentially lethal infection caused by this virus arise from the initial viral infection and the subsequent host inflammatory response. The latter may lead to excessive release of pro-inflammatory cytokines, IL-6 and IL-8, as well as TNF-α ultimately culminating in hypercytokinemia ("cytokine storm"). To address this immuno-inflammatory pathogenesis, multiple clinical trials have been proposed to evaluate anti-inflammatory biologic therapies targeting specific cytokines. However, despite the obvious clinical utility of such biologics, their specific applicability to COVID-19 has multiple drawbacks, including they target only one of the multiple cytokines involved in COVID-19's immunopathy. Therefore, we set out to identify a small molecule with broad-spectrum anti-inflammatory mechanism of action targeting multiple cytokines of innate immunity. In this study, a library of small molecules endogenous to the human body was assembled, subjected to in silico molecular docking simulations and a focused in vitro screen to identify anti-proinflammatory activity via interleukin inhibition. This has enabled us to identify the loop diuretic furosemide as a candidate molecule. To pre-clinically evaluate furosemide as a putative COVID-19 therapeutic, we studied its anti-inflammatory activity on RAW264.7, THP-1 and SIM-A9 cell lines stimulated by lipopolysaccharide (LPS). Upon treatment with furosemide, LPS-induced production of pro-inflammatory cytokines was reduced, indicating that furosemide suppresses the M1 polarization, including IL-6, TNF- α and IL-1 β release. In addition, we found that furosemide promotes the production of anti-inflammatory cytokine products (IL-1RA, arginase), indicating M2 polarization. Accordingly, we conclude that furosemide is a reasonably potent inhibitor of IL-6 and TNF- α that is also safe, inexpensive and well-studied. Our pre-clinical data suggest that it may be a candidate for repurposing as an inhaled therapy against COVID-19.

¹ Krembil Research Institute, University Health Network, Toronto, Ontario, Canada

Faculty of Pharmacy, University of Toronto, Toronto, Ontario, Canada

³ Faculty of Medicine, University of Toronto, Toronto, Ontario, Canada



Furosemide as a Possible Therapeutic for COVID-19

Zhiyu Wang ^{1,2} , Yanfei Wang ¹ , Prachi Vilekar ¹ , Seung-Pil Yang ¹ , Mayuri Gupta ¹ , Myong In Oh ¹
Autumn Meek ¹ , Lisa Doyle ¹ , Anja Brennecke ¹ , Imindu Liyanage ^{1,3} , Mark Reed ¹ , Christopher
Barden ¹ , Donald F. Weaver ^{1,2,3}
¹ Krembil Research Institute, University Health Network, Toronto, Canada
² Faculty of Pharmacy, University of Toronto, Ontario, Canada
³ Faculty of Medicine, University of Toronto, Ontario, Canada
Corresponding author: Donald F. Weaver ¹
Email address: dweaver@uhnres.utoronto.ca



Abstract

The novel coronavirus SARS-CoV-2 has become a global health concern. The morbidity
and mortality of the potentially lethal infection caused by this virus arise from the initial viral
infection and the subsequent host inflammatory response. The latter may lead to excessive
release of pro-inflammatory cytokines, IL-6 and IL-8, as well as TNF- α ultimately culminating
in hypercytokinemia ("cytokine storm"). To address this immuno-inflammatory pathogenesis,
multiple clinical trials have been proposed to evaluate anti-inflammatory biologic therapies
targeting specific cytokines. However, despite the obvious clinical utility of such biologics, their
specific applicability to COVID-19 has multiple drawbacks, including they target only one of the
multiple cytokines involved in COVID-19's immunopathy. Therefore, we set out to identify a
small molecule with broad-spectrum anti-inflammatory mechanism of action targeting multiple
cytokines of innate immunity. In this study, a library of small molecules endogenous to the
human body was assembled, subjected to in silico molecular docking simulations and a focused
in vitro screen to identify anti-pro-inflammatory activity via interleukin inhibition. This has
enabled us to identify the loop diuretic furosemide as a candidate molecule. To pre-clinically
evaluate furosemide as a putative COVID-19 therapeutic, we studied its anti-inflammatory
activity on RAW264.7, THP-1 and SIM-A9 cell lines stimulated by lipopolysaccharide (LPS).
Upon treatment with furosemide, LPS-induced production of pro-inflammatory cytokines was
reduced, indicating that furosemide suppresses the M1 polarization, including IL-6, TNF- α and
IL-1 β release. In addition, we found that furosemide promotes the production of anti-
inflammatory cytokine products (IL-1RA, arginase), indicating M2 polarization. Accordingly,
we conclude that furosemide is a reasonably potent inhibitor of IL-6 and TNF- α that is also safe,
inexpensive and well-studied. Our pre-clinical data suggest that it may be a candidate for
repurposing as an inhaled therapy against COVID-19.



Introduction

41	COVID-19, a potentially lethal infection caused by the SARS-CoV-2 virus, has emerged as a
42	public health crisis of global concern. Currently, there are no effective curative treatments for
43	COVID-19, affording little patient recourse beyond supportive care (Cortegiani et al. 2020). The
44	morbidity and mortality of COVID-19 arise from two competing pathological processes, the
45	initial viral infection and the subsequent host inflammatory response, the latter of which may
46	lead to excessive release of pro-inflammatory cytokines (interleukins [e.g. IL-6, IL-8] or non-
47	interleukins [e.g. TNF-α]), and may culminate in hypercytokinemia ("cytokine storm"), a self-
48	targeting inflammatory response syndrome (Conti et al. 2020; Mehta et al. 2020; Qin et al. 2020;
49	Huang et al. 2020). Reflecting these dichotomous disease processes, current therapeutic
50	development strategies may be categorized into two broad groups: anti-viral and anti-
51	inflammatory. Arguably, truly effective treatments may require both agents, since an antiviral
52	will fail to suppress uncontrolled pro-inflammatory cytokine release once the process has been
53	triggered.
54	To address the COVID-19 immuno-inflammatory pathogenesis, multiple clinical trials
55	have been proposed to evaluate anti-inflammatory biologic therapies targeting specific cytokines.
56	Agents under consideration include tocilizumab (Peking University First Hospital 2020; Tongji
57	Hospital et al. 2020; National Cancer Institute N 2020) and sarilumab (Pharmaceuticals R and
58	Sanofi 2020), both monoclonal antibodies that target the IL-6 pathway (Sebba 2008; Boyce et al.
59	2018), as well as adalimumab, which binds with specificity to TNF- α (Furst <i>et al.</i> 2003).
60	Preliminary data from a Chinese study in which tocilizumab was given to 21 patients with severe
61	COVID-19 reported that the patients "improved remarkably" with 19 patients being discharged
62	13.5 days following treatment, and the remainder "recovering well" (Xu X et al. 2020).



However, despite the obvious clinical utility of such biologics for many disorders, their specific applicability to COVID-19 is hampered by various issues: they target only one of the multiple cytokines implicated in COVID-19's immunopathy; if administered systemically, they can predispose patients to secondary infections or other toxicities, such as hepatoxicity; and they may be expensive to mass produce and distribute. Therefore, they are of limited utility in the context of a global pandemic.

Accordingly, we set out to identify a small molecule with the following properties: broad-spectrum anti-inflammatory mechanism of action targeting cytokines of innate immunity; low toxicity and excellent safety profile; chemically stable; easily stored and administered; able to be rapidly adopted in clinical settings worldwide; and, widespread availability with inexpensive and efficient means of production. As described herein, a systemic series of *in silico* and *in vitro* studies have enabled us to identify furosemide as a candidate molecule.

Materials & Methods

77 In Silico Studies

- Molecular docking simulations: Molecular docking simulations on the endogenous
 molecule (1136) and known drug datasets (1768) against II-6 and TNF-α were carried out in two
 steps. The first step involved placement of the endogenous or ligand molecule in an identified
 binding pocket (docking) of IL-6 and TNF-α. In second step, the calculation of the binding
 energies of the docked molecules (scoring) was completed.
- Preparation of TNF-α and IL-6 3D protein structures: The TNF-α structure (PDB code:
 2AZ5) and IL-6 structure (PDB code: 1ALU) were loaded into Molecular Operating
- 85 Environment (MOE 2019.0101) software (MOE, 2019). The loaded crystal structure was



86 prepared employing the 'QuickPrep Panel' in MOE, which contains the 'structure preparation' feature. The 'Protonate3D' function was used to optimize ionization states of the added hydrogen 87 atoms. Water molecules, which were present 4.5 Å away from ligand or receptor, were deleted. 88 The MFF94x force field, with RMS gradient of 0.05 kcal/Å, was used for energy minimization 89 90 (Panigrahi & Desiraju 2007). A Ramachandran plot was used to confirm the geometric and 91 stereochemical qualities of the TNF- α and IL-6 protein structures. 92 Endogenous molecules and known drugs dataset curation: The datasets of endogenous molecules (1136) and drugs (1768) were prepared using MOE software. Two functions 'wash at 93 94 dominant pH of 7.4' and 'energy minimize' were used to obtain an energy minimized molecular form of molecules present at pH 7.4. 95 96 **Binding site selection and docking simulations:** The active site of IL-6 and TNF-alpha 97 was identified using the 'MOE-site Finder' module. The 'Triangle Matcher' placement method and 'London dG' scoring functions were used for docking simulations. The poses from ligand 98 99 conformations were generated in the Placement phase. After placement of poses, the refinement 100 was done with the 'GBVI/WSA dG' scoring method using 'induced fit' option. Induced fit refinement allows both the ligand molecule and protein active site to move freely to facilitate 101 102 residue alignment during docking simulations. Thirty docked poses of placement retention 103 simulation and 10 poses of refinement step were retained. The docking pose corresponding to the 104 highest score for an endogenous or a drug molecule was considered for comparison of binding 105 affinity within datasets. Further details of descriptor calculation and docking simulations are 106 provided in our recent publications (Gupta et al. 2019; Gupta et al. 2020) and in supporting information. 107

In Vitro Studies

108



110

111

112

113

114

115

116

117

118

119

120

121

122

123

124

125

126

127

128

129

130

131

Inflammation activation on RAW264.7 macrophage: RAW264.7 cells were purchased from ATCC and maintained in Dulbecco's Modified Eagle's Medium (DMEM) containing fetal bovine serum (FBS) at a final concentration of 10%. RAW264.7 cells were seeded in 12-well plates at 0.25 x 10⁶ cells/well seeding density, one day before experiments. To activate the cells, cell culture medium was changed to a lipopolysaccharide (LPS) and Interferon y (IFNy) containing medium with dimethyl sulfoxide (DMSO) or furosemide at required concentrations, followed by 24 h incubation at 37 °C; conditioned media and lysates were harvested for analysis. Inflammation activation on THP-1 monocytic cells: THP-1 cells (ATCC) were maintained in RPMI 1640 medium supplemented with 2-mercaptoethanol at a final concentration of 0.05 mM and FBS at a final concentration of 10%. THP-1 cells were seeded in each well of a 12-well tissue culture plate at a density 0.5 x 10⁶ cells/mL, one day before experiments. THP-1 monocytes were differentiated by 150 nM PMA (phorbol 12-myristate 13-acetate) for 24 h. Cells were then treated with LPS+IFNy with DMSO or furosemide at the required concentration, followed by 48 h incubation; conditioned media and lysates were collected for analysis. Nitric oxide (NO) production by Griess assay: Nitric oxide production from the conditioned media of RAW264.7 and SIM-A9 cell cultures was examined by a Griess assay. Conditioned medium and sulfanilamide were mixed in a microwell plate to form a transient diazonium salt. Then, N-naphtyl-ethylenediamine was added to all wells to form a stable azo compound by incubating for 5-10 min in a dark at room temperature. The absorbance was measured between 520 nm and 550 nm. The concentration of NO production was quantified by being plotted against a standard curve. Enzyme-linked immunosorbent assay (ELISA): Cytokines were quantified using ELISA kits following the manufacturer's instructions. Briefly, the high-binding plates were



132	coated at 100 μ L/well with diluted capture antibodies (1:250) at 4°C overnight. The coated plates
133	were then blocked with the diluent for 1 h before assay. Each sample was diluted accordingly
134	and added to the plates for a 2 h incubation period at room temperature. Plates were then washed
135	with 250 $\mu L/well$ PBS with 0.05% Tween-20 and incubated with detection antibodies (1:250 in
136	assay diluent) for 1 h at room temperature. After another washing step, 1:250 diluted avidin-HRP
137	(horseradish peroxidase) was added and incubated for 30 min. Next, 100 μL TMB-substrate
138	(3,3',5,5'-tetramethylbenzidine) was added and the plate was incubated in dark until the signal
139	was sufficiently developed. The reaction was stopped with 50 μL of 2 N sulfuric acid.
140	Absorbance was measured at 450 nm with a correction of 570 nm using a plate reader.
141	Western blotting: Cells were washed twice with ice-cold PBS and harvested in RIPA
142	buffer supplemented with a protease inhibitor cocktail. The whole-cell extracts were then
143	centrifuged at 22,000 xg for 20 min at 4 °C to remove cell debris. Protein concentrations were
144	quantified using a Micro BCA protein assay kit. The absorbance was measured at 595 nm using
145	a microplate reader. Equal amounts of cellular protein were separated by sodium dodecyl sulfate-
146	polyacrylamide gel electrophoresis (SDS-PAGE) and transferred onto polyvinylidene difluoride
147	(PVDF) membranes at 100 V for 90 min. The membranes were blocked for 1 h in Tris-buffered
148	saline (TBS), pH 7.4, with 0.1% Tween-20 (TBS-T) containing 10% skim milk. The membrane
149	blot was then incubated overnight at 4 $^{\circ}$ C with primary antibodies against iNOS (1:1000), IL-1 β
150	(1:1000), actin (1:5000) and GAPDH (1:5000) in TBS-T containing 5% skim milk. The
151	membrane was washed with TBS-T 3 x 10 mins and incubated with goat anti-rabbit IgG-
152	horseradish peroxidase (1:5,000) for 1 hour. After the washing step, the immunoblotting was
153	visualized by chemiluminescence HRP-substrate.



Flow cytometry: Cells were harvested and re-suspended with staining buffer. Cells were stained with antibody (1:100) by incubating at 4 °C for 30 min in the dark. Stained cells were centrifuged, and the supernatant was discarded. The cell pellets were then re-suspended in cell flow buffer, transferred to FACS tubes and analyzed by flow cytometry within 48 h. To all cells in the experiment, Fc blocker was added.

Inflammation activation on SIM-A9 cells: SIM-A9 (ATCC) cells were maintained in Dulbecco's modified eagle medium: nutrient mixture F-12 (DMEM-F12) with 10% fetal bovine serum, 5% horse-serum and antibiotic-antimycotic. SIM-A9 cells were seeded 24 h before the experiment. Culturing medium was replaced with DMEM-F12 medium containing 5% FBS + 2.5% horse serum with required LPS concentration (final volume is 1 mL/well). The conditioned media and lysates were harvested for cytokine and cell marker examination.

Statistical analysis: Data are presented as mean \pm SD or \pm SEM. Statistical analysis was performed with GraphPad Prism software version 6.01c, applying a two-tailed unpaired t-test. A *p*-value of >0.05 was considered significant.

Results

Identifying an Initial Hit

A screening strategy was devised for identifying an initial compound with potential broadspectrum anti-inflammatory activity targeting relevant cytokines of the pulmonary innate
immune system. Since immunologically-mediated inflammatory responses in the human body
are subject to tight homeostatic regulation, there exist multiple endogenous compounds capable
of either up- or down-regulation of innate immune processes. Accordingly, we sought to identify
an endogenous compound as an initial molecular platform around which to devise a therapeutic.

A library of 1,136 small molecules endogenous to the human body was assembled, subjected to



in silico molecular docking simulations and a focused in vitro screen to identify anti-pro-

inflammatory activity via interleukin inhibition.

Multiple compounds within the tryptophan metabolic pathway were identified, both indoleamine and anthranilate metabolites. In particular, 3-hydroxyanthranilic acid (3-HAA) was found to demonstrate significant anti-inflammatory potential (in accord with previous studies by others, such as Lee *et al.* (2013), who have shown significant activity of 3-HAA in inhibiting IL-6 and TNF- α). Regrettably, 3-HAA is a small polar molecule with poor drug-like properties and is not an approved therapeutic for human use.

Converting Hit to Drug-Like Anthranilate Compound

The task of converting 3-HAA to a drug or drug-like compound can be addressed via two approaches: 1) synthesis of new chemical entities with drug-like properties based on the 3-HAA scaffold, or 2) identification of known drugs with structural properties similar to the 3-HAA scaffold with the goal of repurposing. Because of the urgency imposed by the unfolding pandemic, approach 2 was selected to provide a short-term solution.

Accordingly, 1,768 known drugs were computationally evaluated for anthranilate structural components. This screen identified mefenamic acid (N-(2,3-xylyl)-anthranilate) and furosemide (4-chloro-5-sulfamoyl-N-furfuryl-anthranilate) as the two strongest leads. Mefenamic acid is known to provide significant protection against elevated levels of TNF- α and IL-1 β in radiation-induced genotoxicity of human lymphocytes (Armagan *et al.* 2012; Hosseinimehr *et al.* 2015); furosemide is known to significantly reduce production of IL-6, IL-8, and TNF- α in bronchial inflammation of asthma (Prandota 2002; Yuengsrigul *et al.* 1999). This screen also identified other loop diuretics structurally related to 3-HAA and furosemide, including



bumetanide, piretanide and azosemide (Fig. 1). Arising from the observation that furosemide can reduce bronchial inflammation, can be administered by inhalation (*vide infra*, Discussion) (Prandota 2002; Inokuchi *et al.* 2014; Waskiw-Ford *et al.* 2018). and is a widely available drug, furosemide was selected to be explored for repurposing in the treatment of COVID-19. Furosemide has been used worldwide for decades as a loop diuretic working via the renal Na⁺/K⁺-ATP shuttle pathway.

In Vitro Assessment of Lead Anthranilate Compound

To pre-clinically evaluate furosemide as a putative COVID-19 therapeutic, a series of *in vitro* efficacy assessments was performed to investigate its anti-inflammatory properties. First, we investigated if furosemide could reduce the release of pro-inflammatory cytokines induced by LPS in macrophage cell line. RAW264.7 macrophages were stimulated with LPS in the presence or absence of furosemide and the level of TNF- α and NO were measured from the conditioned media using ELISA and Griess assay, respectively. The results in Fig. 2 (A) and (B) show that LPS induces the production of NO and TNF- α , indicating macrophage polarization to an M1 pro-inflammatory phenotype. When cells were treated with LPS in the presence of 25 μ M of furosemide, the production of NO and TNF- α significantly decreased. To further investigate the reduction of NO production by furosemide, we determined the expression level of inducible nitric oxide synthase (iNOS) which produces NO in response to inflammatory stimulations. We stimulated RAW264.7 macrophages with LPS and IFN γ . The expression of the iNOS was significantly induced by stimulation with LPS and IFN γ , as shown by the Western blot results in Fig. 2 (C). We found that furosemide was able to suppress the expression of iNOS during LPS



and IFN γ induced stimulation. Densitometry analysis showed that normalized iNOS/GAPDH ratio was reduced from 1 to 0.88 by furosemide.

LPS is recognized by the cell surface pattern-recognition receptors such as the toll-like receptor 4 protein (TLR4) and triggers downstream signaling pathways. LPS induces expression of the pro-inflammatory cytokine IFNγ. IFNγ is known to increase TLR4 expression which may then promote the response to LPS stimulation. We investigated the effect of furosemide on LPS-induced TLR4 expression in RAW264.7 macrophage cells using flow cytometry. As shown in Fig. 3, LPS increased the TLR4+ cell population significantly. Whereas IL-4, an anti-inflammatory cytokine, barely induced TLR expression from the cells. Interestingly, furosemide completely blocked LPS-induced TLR4 expression, suggesting the possible involvement of furosemide in the LPS- or IFNγ-induced inflammation.

As the next stage of macrophage activation, we studied the activity of furosemide on the expression and secretion of IL-1β which plays a key role in modulating inflammatory response, as a downstream pro-inflammatory marker of the TLR4 signalling pathway by using differentiated THP-1 monocytes. We analyzed the expression of IL-1β precursor protein (pro-IL-1β) and the secretion of mature IL-1β from THP-1 macrophage cells by using Western blot analysis and ELISA, respectively. Furosemide, as shown in Fig. 4, significantly decreases the expression of pro-IL-1β in differentiated THP-1 cells as identified by Western blot analysis. As the secreted form, we measured soluble IL-1β from the conditioned medium of cell culture via ELISA. The differentiated THP-1 macrophages secrete IL-1β upon LPS stimulation and the amount of secreted IL-1β slightly decreased with co-treatment of LPS with furosemide, demonstrating yet another inflammatory cytokine targeted by furosemide.



To further explore the effect of furosemide on different macrophages, we next tested it on
SIM-A9 cells. We stimulated SIM-A9 macrophages with LPS and analyzed the release of pro-
inflammatory markers such as NO, IL-6 and TNF- α . The results in Fig. 5 show that LPS induced
the production of NO, IL-6 and TNF- α from SIM-A9 cells. Similar to RAW264.7 cell results,
furosemide significantly reduced the production of all these pro-inflammatory markers from
SIM-A9 cells as well.

We have tested three different macrophage cell lines for the effects of furosemide on proinflammatory markers. Furosemide consistently reduced pro-inflammatory markers such as NO production, secretion of IL-6, TNF- α and IL-1 β from different macrophage cell lines, implying that furosemide has broad inhibitory activity against pro-inflammatory cytokines.

Then, we evaluated if furosemide exhibits any effects on anti-inflammatory cytokines. We measured the levels of anti-inflammatory cytokines from the conditioned medium of differentiated THP-1 cells after 48 h of stimulation with LPS and IFNγ by Multiplex assay using flow cytometry. Furosemide induces the expression of IL-4, interleukin-1 receptor antagonist (IL-1RA) and arginase, which are anti-inflammatory markers, suggesting the polarization of THP-1 macrophage to an M2 phenotype (Fig. 6).

Together with the experiments discussed above, these results show that furosemide inhibits the expression of M1 pro-inflammatory markers and promotes the expression of M2 anti-inflammatory markers. Thus, furosemide is a broad-spectrum anti-inflammatory drug candidate targeting multiple cytokines.

In Silico Mechanism of Action Simulations



266 The molecular mechanism of action whereby 3-HAA and furosemide inhibit IL-6 and TNF-α activity is unknown at this time and lies outside the scope of the present study. Interestingly, in 267 an in silico screen of possible binding sites for 3-HAA and related drug anthranilates, we noted 268 favourable interactions with both the IL-6 and TNF-α proteins. Whilst it is improbable that such 269 270 interactions are completely responsible for the observed anti-inflammatory effects, this notable 271 observation is worthy of future experimental evaluation. These computational simulations are briefly outlined below. 272 The binding of 3-HAA in IL-6 and TNF- α active sites is presented in Figs. 7 and 8. The 273 274 docking score (S) of minimum energy pose of 3-HAA in IL-6 is -4.620, and in TNF- α is -4.487. In Figs. 7 (A) and 8 (A), the ligand 3-HAA is shown in yellow and amino acid residues of 275 binding pocket have been labelled. Figures 7 (B) and 8 (B) represent the ligand interaction 276 277 diagrams of 3-HAA with active site residues of TNF-α and IL-6. Figures 9 and 10 present docking simulations of furosemide with TNF- α and IL-6, 278 respectively. In Figs. 9 (A) and 10 (A), furosemide is shown in yellow and the amino acid 279 280 residues of the binding site are labelled. The TNF-α protein complex (PDB: 2AZ5) contains four identical chains having 148 amino acids each and two bound ligands. The A and B chains were 281 282 retained (coloured orange and purple) and co-crystalized; the ligand was removed while 283 preparing the protein structure for docking. 284 Figure 9 (A) shows the minimum energy docking pose of furosemide in the TNF- α active 285 site. The amino acid residues Leu B57, Tyr B59, Gly B121, Tyr A151, Tyr A119 and Leu A120 are involved in forming hydrogen bonding and π - π interactions (arene-arene, arene-H, arene-286

cation) with furosemide in minimum energy docked poses. The docking score of the minimum



energy pose is -6.0854, which indicating that furosemide fits well into the active site of TNF-α
 and inhibits its activity.

Figure 10 shows the minimum energy docking pose of furosemide in the protein structure of human IL-6 (PDB: 1ALU), having 186 amino acid residues and a co-crystallized ligand (tartaric acid). The co-crystallized ligand had been removed during the structure preparation step of the IL-6 protein. Furosemide interacts with Arg 182, Gln 175, Leu 33 and Arg 179 in most of the minimum energy poses. The docking score (S) of the minimum energy pose of furosemide with IL-6 is -5.1343, which computationally supports the ability of furosemide to inhibit IL-6 activity.

Discussion

The pathogenic mechanisms of COVID-19 morbidity and mortality are diverse, though immuno-inflammatory contributions are likely a central player. It is now appreciated that COVID-19 afflicted individuals with major respiratory symptoms have pathologically elevated levels of proinflammatory cytokines including IL-6, IL-8 and TNF-α (Conti *et al.* 2020; Mehta *et al.* 2020; Qin *et al.* 2020; Huang *et al.* 2020). A logical therapeutic approach to the management of COVID-19 thus includes a need to modulate immunotoxicity.

Tryptophan and its metabolites, particularly via the indoleamine-2,3-dioxygenase initiated pathway, have a previously described role as endogenous modulators of innate immunity. Of these various metabolites, 3-HAA has been identified to exhibit a significant anti-inflammatory ability to suppress inflammation mediated via multiple pro-inflammatory interleukin cytokines, including IL-1β, IL-6, IL-8 and TNF-α (Lee *et al.* 2013). This motivated our search for an anthranilate-based 3-HAA-like agent from a library of known drugs; furosemide emerged as a possible candidate from this search.



312

313

314

315

316

317

318

319

320

321

322

323

324

325

326

327

328

329

330

331

332

333

As part of its pre-clinical evaluation, we studied furosemide's anti-inflammatory activity on multiple macrophage cell lines involved in innate immunity. Broadly conceptualized stimulated macrophages can be polarized to either an M1 pro-inflammatory phenotypes or an M2 anti-inflammatory phenotype. We investigated if furosemide inhibits the production of proinflammatory cytokines (M1) or promotes the secretion of anti-inflammatory cytokines (M2) involved in COVID-19 disease progression, using RAW264.7, THP-1 and SIM-A9 cell lines. Upon stimulation, these cell lines initiate an immune response by producing cellular stress signals and pro-inflammatory cytokines. Upon treatment with furosemide, these proinflammatory markers were reduced, indicating that furosemide suppresses the M1 polarization, including NO, IL-6, TNF-α and IL-1β. More importantly, our Multiplex ELISA results demonstrate furosemide promotes the production of anti-inflammatory cytokine products (IL-1RA, arginase), indicating M2 polarization. Furosemide is a small molecule with a molecular weight of 330.75 g/mol and relatively low lipophilicity (logP = 2.03) (Hardman *et al.* 2001). Although the drug has low water solubility at pH 7, furosemide can be formulated in weakly basic buffer solution (pH 8) to achieve 10 mg/mL solutions suitable for intravenous administration. Due to the presence a primary sulfonamide and carboxylic acid group, furosemide is highly bound to albumin with a human plasma protein binding value of $98.6 \pm 0.4\%$. The drug has a very low volume of distribution ($V_D = 0.13 \pm 0.06$ L/kg) and a relatively short half-life of 1.3 ± 0.8 h (Hardman et al. 2001). These pharmacokinetic parameters along with high plasma protein binding equates to low tissue distribution with furosemide being retained with the blood. These intrinsic molecular properties are ideal for targeting macrophages contained within the blood stream prior to their tissue distribution. Furosemide exhibits a large therapeutic window.



335

336

337

338

339

340

341

342

343

344

345

346

347

348

349

350

351

352

353

354

355

356

Furosemide is listed on the WHO's List of "Essential Medicines"; it is readily available worldwide, is easily manufactured, and has a long record of safety and efficacy when given orally or intravenously. More importantly, furosemide may also be administered safely by inhalation. More than 20 years ago, the concept of inhaled furosemide was explored as an approach to reduce dyspnoea, primarily based on the rationale that edematous airway mast cells would be reduced in size following diuresis (Prandota 2002). However, further investigations established that the mechanism of action was not related to local diuretic effect or engagement of the Na⁺/K⁺-ATP shuttle. More recent studies have reported reduction in pulmonary IL-6, IL-8, and TNF-α levels upon administering inhaled furosemide to patients with conditions including tachypnoea (Armed Forces Hospital Pakistan 2016; University of Cologne 2012), bronchopulmonary dysplasia (University of North Carolina et al. 2015), and chronic lung disease (Center BIDM and Research NIoN 2014; McGill University 2016; Oxford Brookes University 2015). A 2018 double-blind, placebo-controlled trial by Grogono et al. (2018) evaluated inhaled nebulized furosemide (40 mg furosemide in 4 mL 0.9% saline), demonstrating improved efficacy after multiple dosing per day with no untoward effects. Therefore, accumulated data indicate that furosemide is a cytokine-targeting anti-inflammatory, which may be safely administered by inhalation multiple times per day. Our *in silico* screening identified other loop diuretics with structural similarities to furosemide. Bumetanide exhibits anti-inflammatory properties in LPS stimulated RAW264.7 cells, reduces LPS-induced production of cytokines following direct pulmonary administration,

furosemide. Bumetanide exhibits anti-inflammatory properties in LPS stimulated RAW264.7 cells, reduces LPS-induced production of cytokines following direct pulmonary administration, and lowers levels of TNF-α production in lung-injured mice (Hung *et al.* 2018). Bumetanide however failed to inhibit sodium metabisulfite induced bronchoconstriction in asthmatic subjects (O'Connor *et al.* 1991). Piretanide and azosemide have also been variously studied in models of



cytokine-mediated inflammation and bronchoconstriction (Yeo *et al.* 1992). Since none of these agents are in widespread clinical use, we have elected to pursue the development of furosemide in COVID-19 because of its worldwide availability in the time of a global pandemic.

The potential use of furosemide in the anti-inflammatory treatment of COVID-19 has strengths and weaknesses. Furosemide is inexpensive and available in every country in the world; it is safe and has profound anti-inflammatory cytokine activity, particularly against IL-6 and TNF-α. If administered orally, furosemide can produce a profound diuresis which would be a clinical detriment in a febrile and potentially dehydrated person. When administered orally, the pharmacokinetics of furosemide indicate that it would have primarily intra-vascular distribution, suggesting greater utility early in the course of the disease, but less so in later-stage ventilator-supported individuals in whom macrophage migration from bloodstream to pulmonary tissue has occurred. As the disease progresses, direct administration of furosemide to the lungs by nebulized delivery adequately addresses the need to have furosemide reach intra-alveolar macrophages. Care must be taken to prevent viral contamination and bystander exposure during the aerosolized administration of the drug, but this can be achieved with appropriate cautions in place. We are currently pursuing a clinical study of inhaled furosemide in people with COVID-19.

Conclusions

COVID-19 is a pandemic threatening global health. The need to identify innovative therapeutics which may be deployed rapidly and efficiently is a pharmacological priority. Furosemide is a safe, inexpensive, well-studied small molecule which is a reasonably potent inhibitor of IL-6 and TNF-α and may be administered locally to the lungs; pre-clinical data from *in silico* and *in vitro*





380	experiments suggest that it may be a candidate for repurposing as an inhaled therapy against the
381	immunopathologies of COVID-19.
382	
383	Supporting Information: A list of physiochemical descriptors used as initial screening test of
384	the dataset; a list of promising drug candidates along with corresponding physiochemical
385	descriptors; Docking Score 'S' of promising drug candidates with IL-6 and TNF- α ; Figures of
386	Mefenamic acid, Bumetanide, Piretanide and Azosemide drugs docking into binding site of
387	TNF- α and IL-6 and Ligand interaction diagram of Mefenamic acid Mefenamic acid,
388	Bumetanide, Piretanide and Azosemide drugs in active site of TNF- α and IL-6. This information
389	is available free of charge on <i>PeerJ</i> .
390	



391 References

- 392 Armagan G, Turunc E, Kanit L, Yalcin A. Neuroprotection by mefenamic acid against D-serine:
- involvement of oxidative stress, inflammation and apoptosis. Free Radic Res. 2012;46(6):726–
- 394 39. doi:10.3109/10715762.2012.669836.
- 395 Armed Forces Hospital Pakistan. Role of Salbutamol and Furosemide in TTN.
- 396 https://ClinicalTrials.gov/show/NCT03208894 2016.
- 397 Boyce EG, Rogan EL, Vyas D, Prasad N, Mai Y. Sarilumab: Review of a Second IL-6 Receptor
- 398 Antagonist Indicated for the Treatment of Rheumatoid Arthritis. Ann Pharmacother.
- 399 2018;52(8):780–91. doi:10.1177/1060028018761599.
- 400 Center BIDM, Research NIoN. Aerosol Inhalation Treatment for Dyspnea Patients.
- 401 https://ClinicalTrials.gov/show/NCT02524054 2014.
- 402 Conti P, Ronconi G, Caraffa A, Gallenga C, Ross R, Frydas I, Kritas S. Induction of pro-
- 403 inflammatory cytokines (IL-1 and IL-6) and lung inflammation by Coronavirus-19 (COVI-19 or
- 404 SARS-CoV-2): anti-inflammatory strategies. J Biol Regul Homeost Agents 2020.
- 405 doi:10.23812/CONTI-E.
- 406 Cortegiani A, Ingoglia G, Ippolito M, Giarratano A, Einav S. A systematic review on the
- 407 efficacy and safety of chloroquine for the treatment of COVID-19. J Crit Care 2020.
- 408 doi:10.1016/j.jcrc.2020.03.005.
- 409 Furst DE, Schiff MH, Fleischmann RM, Strand V, Birbara CA, Compagnone D, et al.
- 410 Adalimumab, a fully human anti tumor necrosis factor-alpha monoclonal antibody, and
- 411 concomitant standard antirheumatic therapy for the treatment of rheumatoid arthritis: results of
- 412 STAR (Safety Trial of Adalimumab in Rheumatoid Arthritis). 2003;30(12):2563–71.
- 413 Grogono JC, Butler C, Izadi H, Moosavi SH. Inhaled furosemide for relief of air hunger versus
- sense of breathing effort: a randomized controlled trial. Respir Res. 2018;19(1):181.
- 415 doi:10.1186/s12931-018-0886-9.
- 416 Gupta M, Lee HJ, Barden CJ, Weaver DF. The Blood-Brain Barrier (BBB) Score. J Med Chem.
- 417 2019;62(21):9824–36. doi:10.1021/acs.jmedchem.9b01220.
- 418 Gupta M, Bogdanowicz T, Reed MA, Barden CJ, Weaver DF. The Brain Exposure Efficiency
- 419 (BEE) Score, ACS Chem Neurosci, 2020;11(2):205–24. doi:10.1021/acschemneuro.9b00650.
- 420 Hardman JG, Goodman LS, Gilman AG, editors. Goodman & Gilman's The pharmacological
- basis of therapeutics. 10th ed. New York, NY: McGraw-Hill Med. Publ; 2001.
- 422 Hosseinimehr SJ, Nobakht R, Ghasemi A, Pourfallah TA. Radioprotective effect of mefenamic
- 423 acid against radiation-induced genotoxicity in human lymphocytes. Radiat Oncol J.
- 424 2015;33(3):256–60. doi:10.3857/roj.2015.33.3.256.
- 425 Huang C, Wang Y, Li X, Ren L, Zhao J, Hu Y, et al. Clinical features of patients infected with
- 426 2019 novel coronavirus in Wuhan, China. The Lancet. 2020;395(10223):497–506.
- 427 doi:10.1016/S0140-6736(20)30183-5.
- 428 Hung C-M, Peng C-K, Wu C-P, Huang K-L. Bumetanide attenuates acute lung injury by
- 429 suppressing macrophage activation. Biochem Pharmacol. 2018;156:60–7.
- 430 doi:10.1016/j.bcp.2018.08.013.



- 431 Inokuchi R, Aoki A, Aoki Y, Yahagi N. Effectiveness of inhaled furosemide for acute asthma
- 432 exacerbation: a meta-analysis. Crit Care. 2014;18(6):621. doi:10.1186/s13054-014-0621-y.
- 433 Lee W-S, Lee S-M, Kim M-K, Park S-G, Choi I-W, Choi I, et al. The tryptophan metabolite 3-
- 434 hydroxyanthranilic acid suppresses T cell responses by inhibiting dendritic cell activation. Int
- 435 Immunopharmacol. 2013;17(3):721–6. doi:10.1016/j.intimp.2013.08.018.
- 436 McGill University. Inhaled Nebulized Furosemide & Physical Activity-Related Breathlessness.
- 437 https://ClinicalTrials.gov/show/NCT01851980 2016.
- 438 Mehta P, McAuley DF, Brown M, Sanchez E, Tattersall RS, Manson JJ. COVID-19: consider
- cytokine storm syndromes and immunosuppression. The Lancet. 2020;395(10229):1033–4.
- 440 doi:10.1016/S0140-6736(20)30628-0.
- 441 Molecular Operating Environment (MOE) 2019.0101; Chemical Computing Group ULC,
- 442 Montreal, QC, Canada, 2019.
- 443 National Cancer Institute N. Tocilizumab in COVID-19 Pneumonia (TOCIVID-19).
- 444 https://ClinicalTrials.gov/show/NCT04317092 2020.
- O'Connor BJ, Chung KF, Chen-Worsdell YM, Fuller RW, Barnes PJ. Effect of inhaled
- 446 furosemide and bumetanide on adenosine 5'-monophosphate- and sodium metabisulfite-induced
- bronchoconstriction in asthmatic subjects. Am Rev Respir Dis. 1991;143(6):1329–33.
- 448 doi:10.1164/ajrccm/143.6.1329.
- 449 Oxford Brookes University. Specificity of Dyspnoea Relief With Inhaled Furosemide.
- 450 https://ClinicalTrials.gov/show/NCT02881866 2015.
- 451 Panigrahi SK, Desiraju GR. Strong and weak hydrogen bonds in the protein-ligand interface.
- 452 Proteins. 2007;67(1):128–41. doi:10.1002/prot.21253.
- 453 Peking University First Hospital. Favipiravir Combined With Tocilizumab in the Treatment of
- 454 Corona Virus Disease 2019. https://ClinicalTrials.gov/show/NCT04310228 2020.
- 455 Pharmaceuticals R, Sanofi. Evaluation of the Efficacy and Safety of Sarilumab in Hospitalized
- 456 Patients With COVID-19. https://ClinicalTrials.gov/show/NCT04315298 2020.
- 457 Prandota J. Furosemide: progress in understanding its diuretic, anti-inflammatory, and
- 458 bronchodilating mechanism of action, and use in the treatment of respiratory tract diseases. Am J
- 459 Ther. 2002;9(4):317–28. doi:10.1097/00045391-200207000-00009.
- 460 Oin C, Zhou L, Hu Z, Zhang S, Yang S, Tao Y, et al. Dysregulation of immune response in
- patients with COVID-19 in Wuhan, China. Clin Infect Dis 2020. doi:10.1093/cid/ciaa248.
- 462 Sebba A. Tocilizumab: the first interleukin-6-receptor inhibitor. Am J Health Syst Pharm.
- 463 2008;65(15):1413-8. doi:10.2146/ajhp070449.
- 464 Tongji Hospital, Hubei Xinhua Hospital, Wuhan No.1 Hospital, Wuhan central hospital.
- Tocilizumab vs CRRT in Management of Cytokine Release Syndrome (CRS) in COVID-19.
- 466 https://ClinicalTrials.gov/show/NCT04306705 2020.
- 467 University of Cologne. Trial on Treatment With Inhaled Furosemide of Preterm and Term
- Neonates With Transient Tachypnoea. https://ClinicalTrials.gov/show/NCT01407848 2012.
- 469 University of North Carolina, Chapel Hill, Duke University, Eunice Kennedy Shriver National
- 470 Institute of Child Health and Human Development, The Emmes Company LLC. Safety of



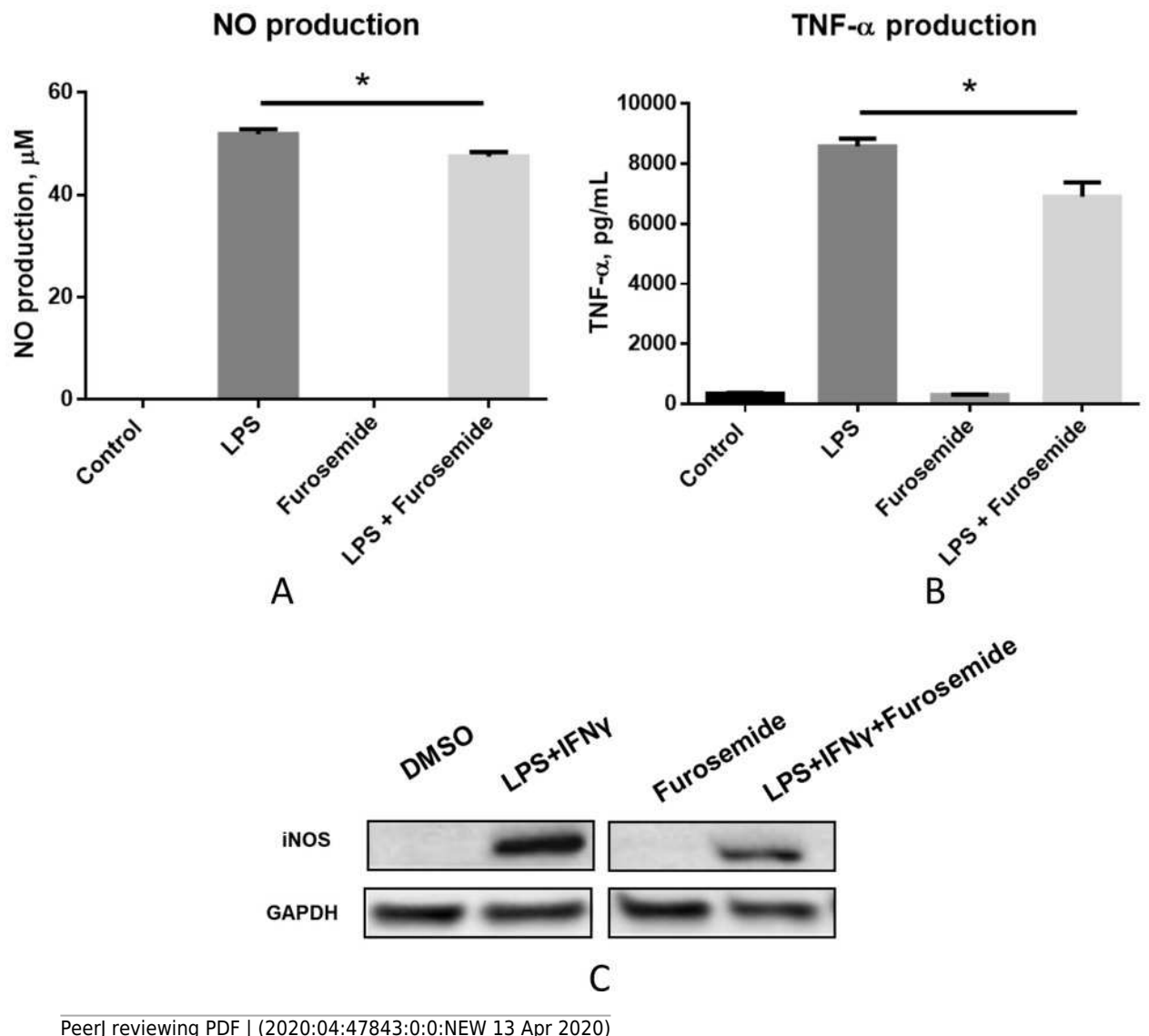
- 471 Furosemide in Premature Infants at Risk of Bronchopulmonary Dysplasia (BPD).
- 472 https://ClinicalTrials.gov/show/NCT02527798 2015.
- 473 Waskiw-Ford M, Wu A, Mainra A, Marchand N, Alhuzaim A, Bourbeau J, et al. Effect of
- 474 Inhaled Nebulized Furosemide (40 and 120 mg) on Breathlessness during Exercise in the
- 475 Presence of External Thoracic Restriction in Healthy Men. Front Physiol. 2018;9:86.
- 476 doi:10.3389/fphys.2018.00086.
- 477 Xu X, Han M, Li T, Sun W, Wang D, Fu B. Effective Treatment of Severe COVID-19 Patients
- 478 with Tocilizumab. ChinaXiv. 202003.000262020 2020.
- 479 Yeo CT, O'Connor BJ, Chen-Worsdell M, Barnes PJ, Chung KF. Protective effect of loop
- 480 diuretics, piretanide and frusemide, against sodium metabisulphite-induced bronchoconstriction
- 481 in asthma. European Respiratory Journal. 1992(5):1184–8.
- 482 Yuengsrigul A, Chin TW, Nussbaum E. Immunosuppressive and cytotoxic effects of furosemide
- on human peripheral blood mononuclear cells. Annals of Allergy, Asthma & Immunology.
- 484 1999;83(6):559–66. doi:10.1016/S1081-1206(10)62870-0.

Loop diuretics structurally related to 3-HAA.

(A) 3-Hydroxyanthranilic acid, (B) furosemide, (C) bumetanide, (D) piretanide and (E) azosemide.

Furosemide decreases the production of NO and TNF- α .

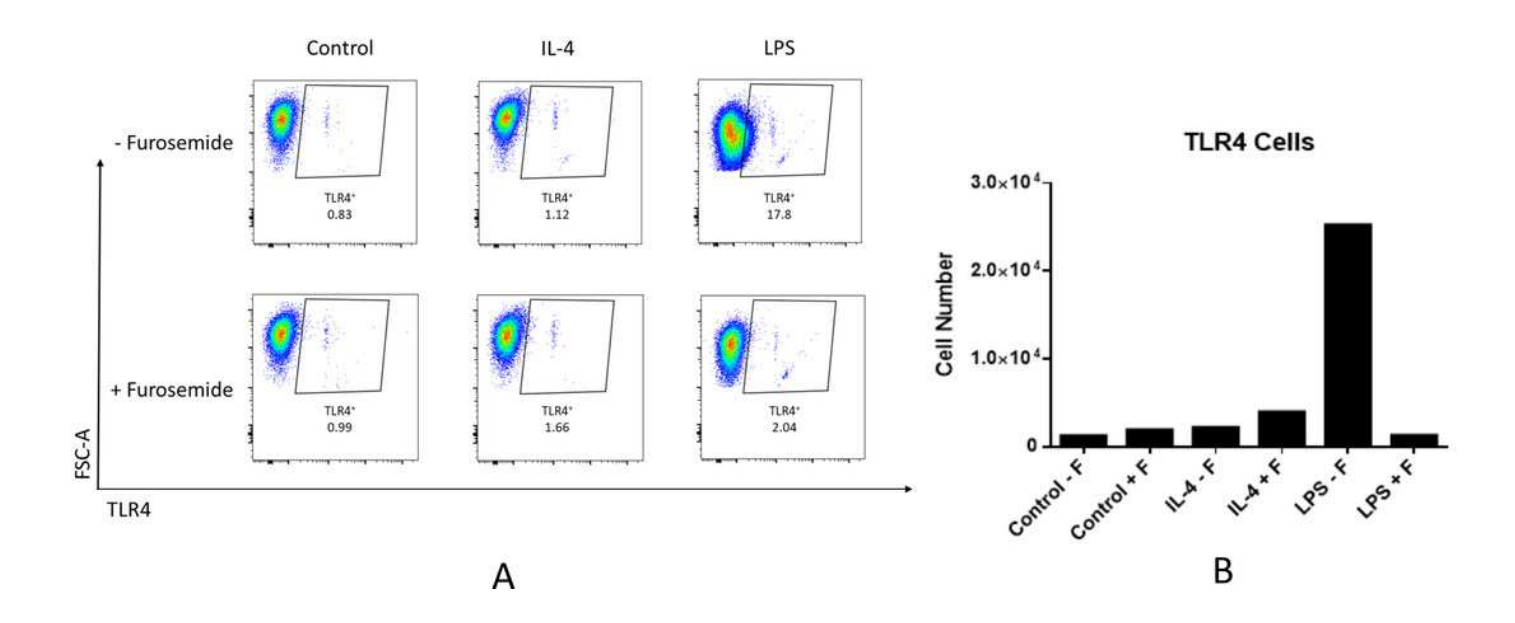
Production of (A) NO and (B) TNF-α from RAW264.7 cells upon LPS induction were determined by Griess assay and ELISA from the conditioned medium. Error bars show SEM, n=3. *, p < 0.05. (C) iNOS expression level from RAW264.7 cells was assessed by Western blot analysis. Cells were treated with LPS+IFNy with DMSO or 25 µM furosemide. After 24h of incubation, cell lysate was harvested for Western blot analysis. GAPDH = Glyceraldehyde 3-phosphate dehydrogenase.





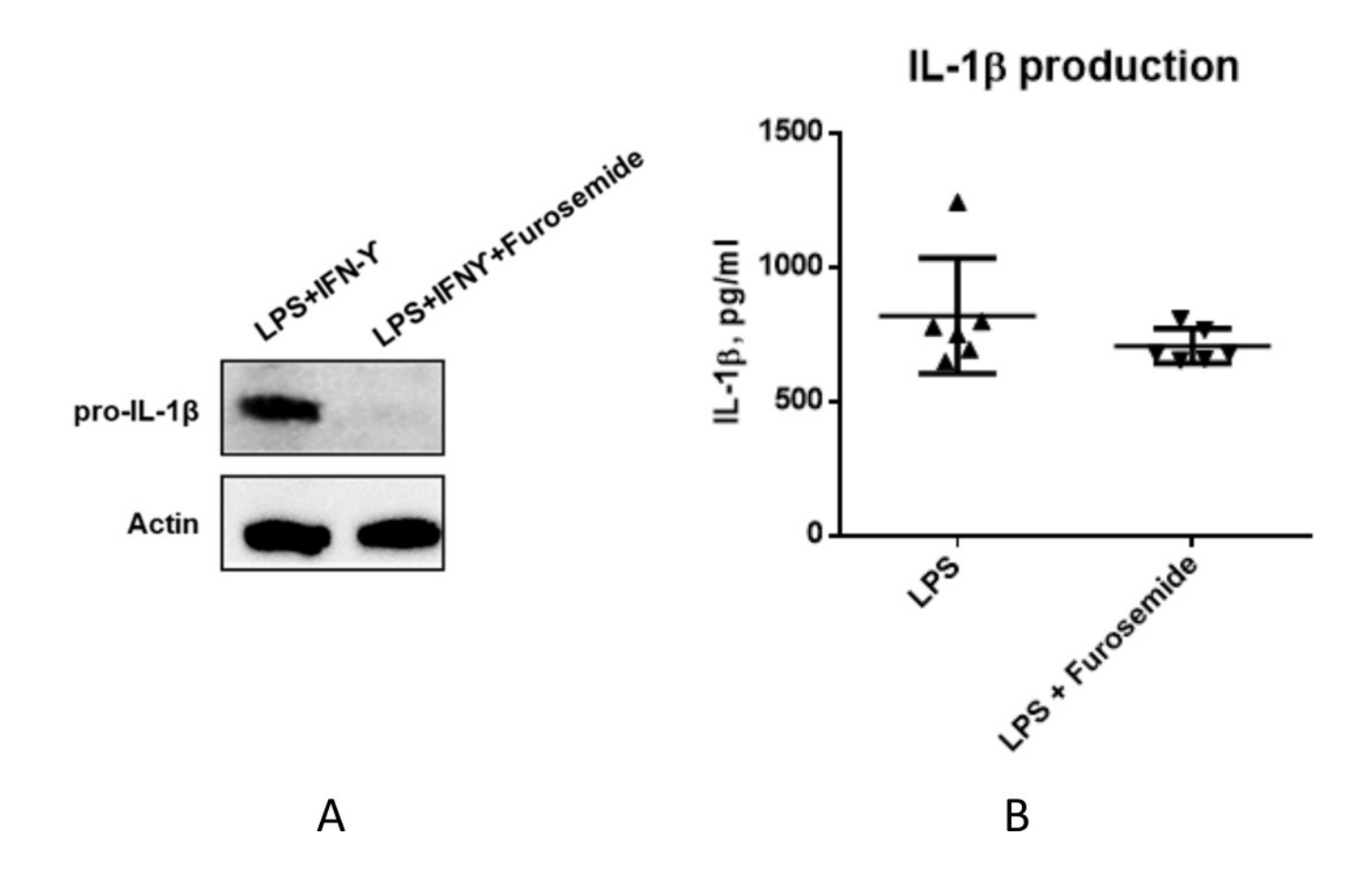
Furosemide significantly decreases TLR4+ cell population.

RAW264.7 macrophage cells were stimulated with LPS and flow cytometry was used to determine TLR4+ cell population. (A), % of Vis and (B), cell numbers for TLR4+. F = furosemide, FSC-A = front scatter.



Furosemide significantly decreases both the expression of pro-IL-1 β and the secretion of IL-1 β from differentiated THP-1 cells.

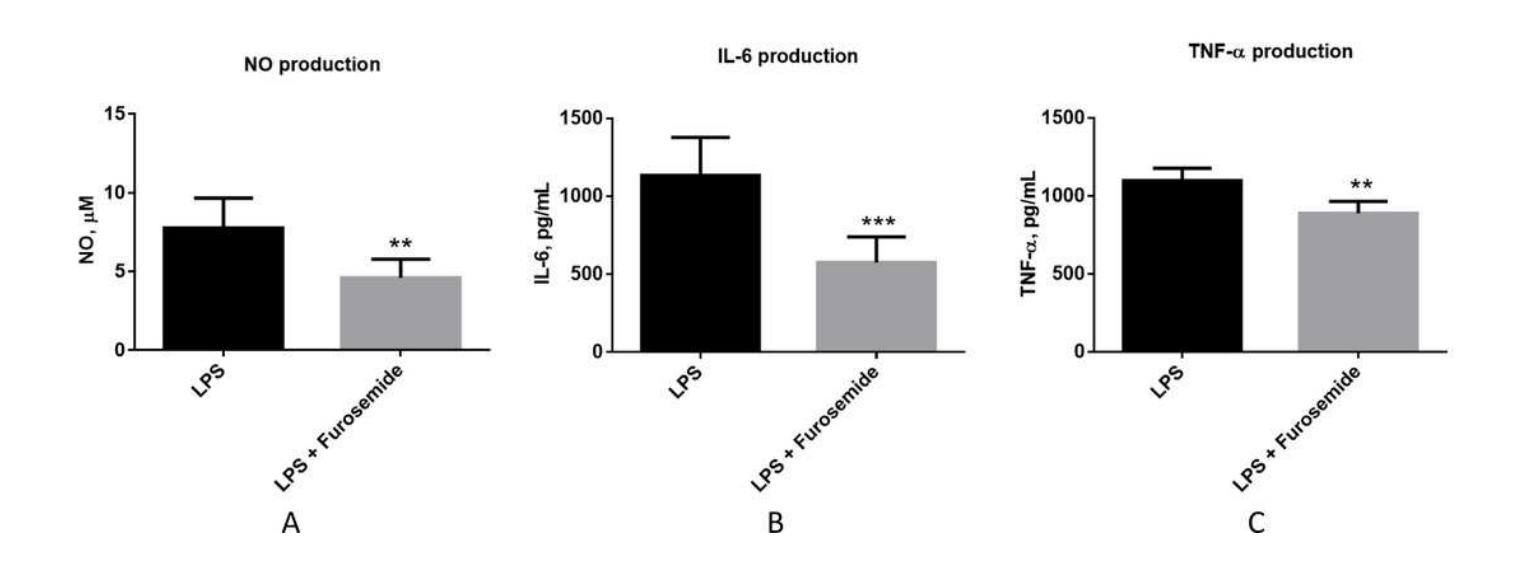
Effect of furosemide on differentiated THP-1 monocytes: (A) Western blot showing the expression of pro-IL-1 β upon treatment with DMSO and furosemide, respectively. Actin was used as a loading control. (B) Concentration of IL-1 β was measured by ELISA from the conditioned medium after treating cells with furosemide, LPS or both. Error bars show SD, n=6.





Furosemide decreases production of pro-inflammatory markers from LPS-stimulated SIM-A9 cells.

Production of (A) NO, (B) IL-6 and (C) TNF α after stimulation with LPS was measured from the conditioned media by either Griess assay or ELISA. Error bars show n=6. **, p < 0.01; ***, p < 0.001.





Furosemide induces expression of anti-inflammatory phenotype markers.

Analysis of the anti-inflammatory markers (A) IL-4, (B) IL-1RA and (C) Arginase from differentiated THP-1 macrophage upon treatment with LPS and INF γ with DMSO or 25 μ M furosemide. After 48h of incubation, conditioned medium was harvested for cytokine analysis. Error bars show SD, n=2. **, p < 0.01.

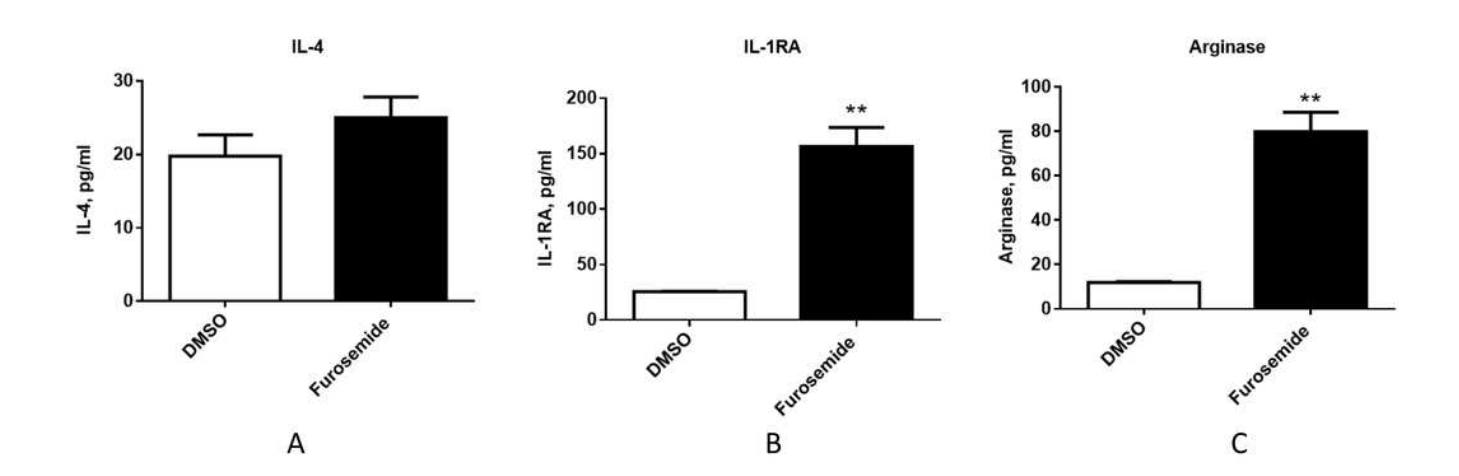
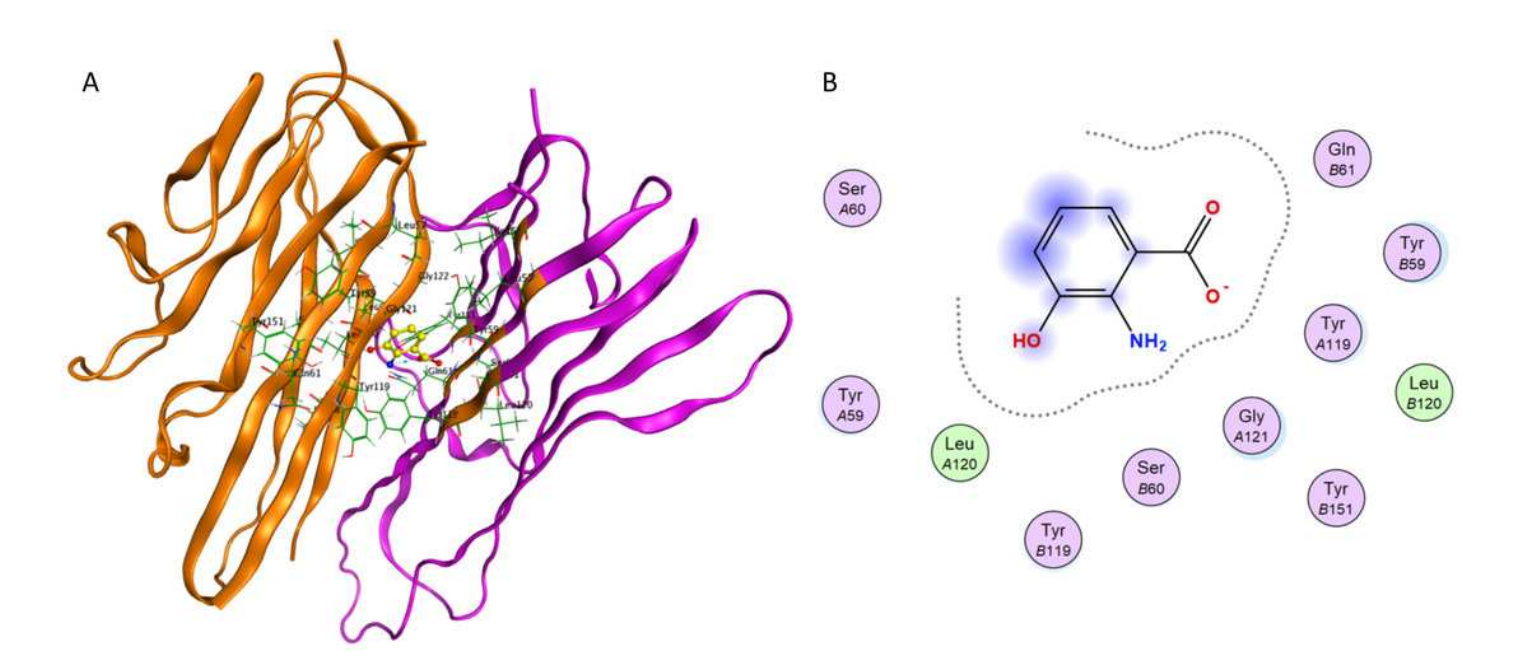




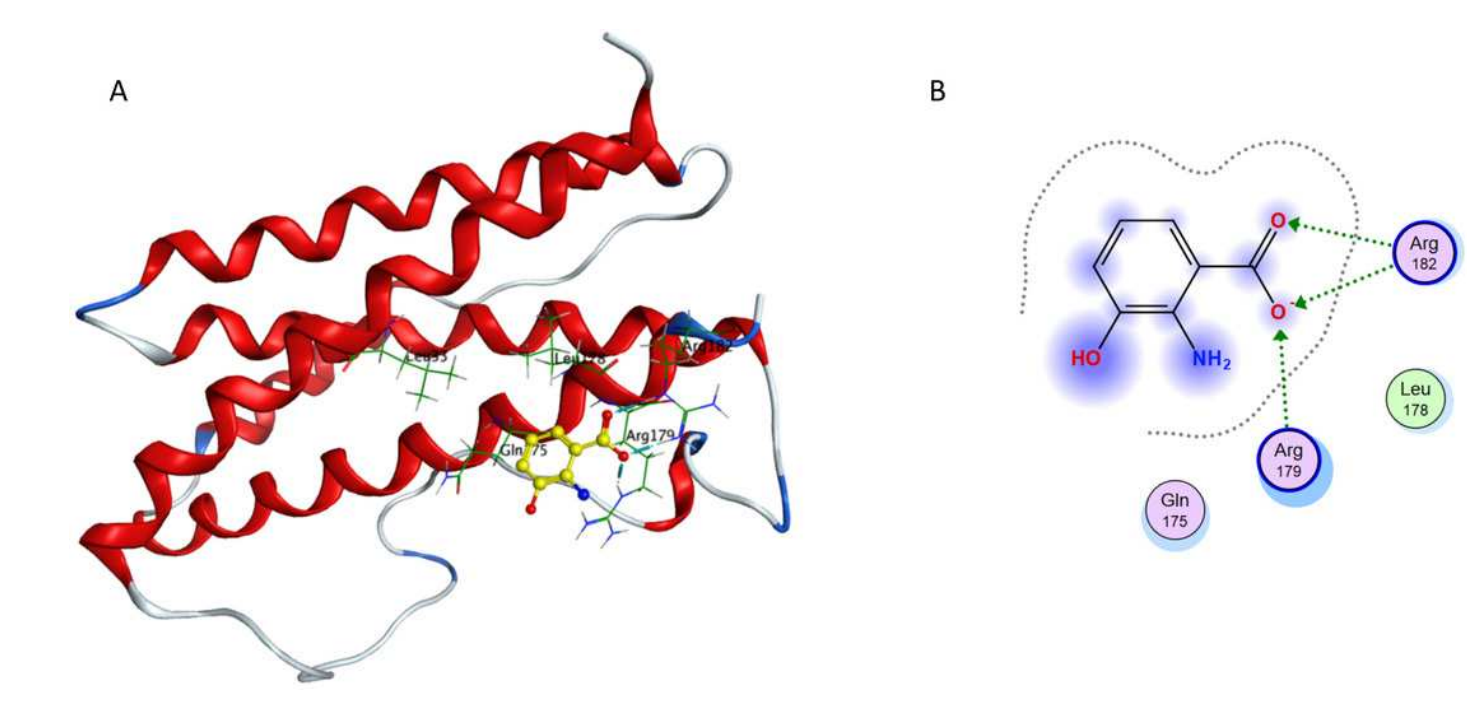
Figure 7 Interaction of 3-HAA with TNF- α active site.

(A) Binding of 3-HAA in the active site of tumor necrosis factor α (TNF- α); (B) Ligand interaction diagram of 3-HAA in binding site of TNF- α .



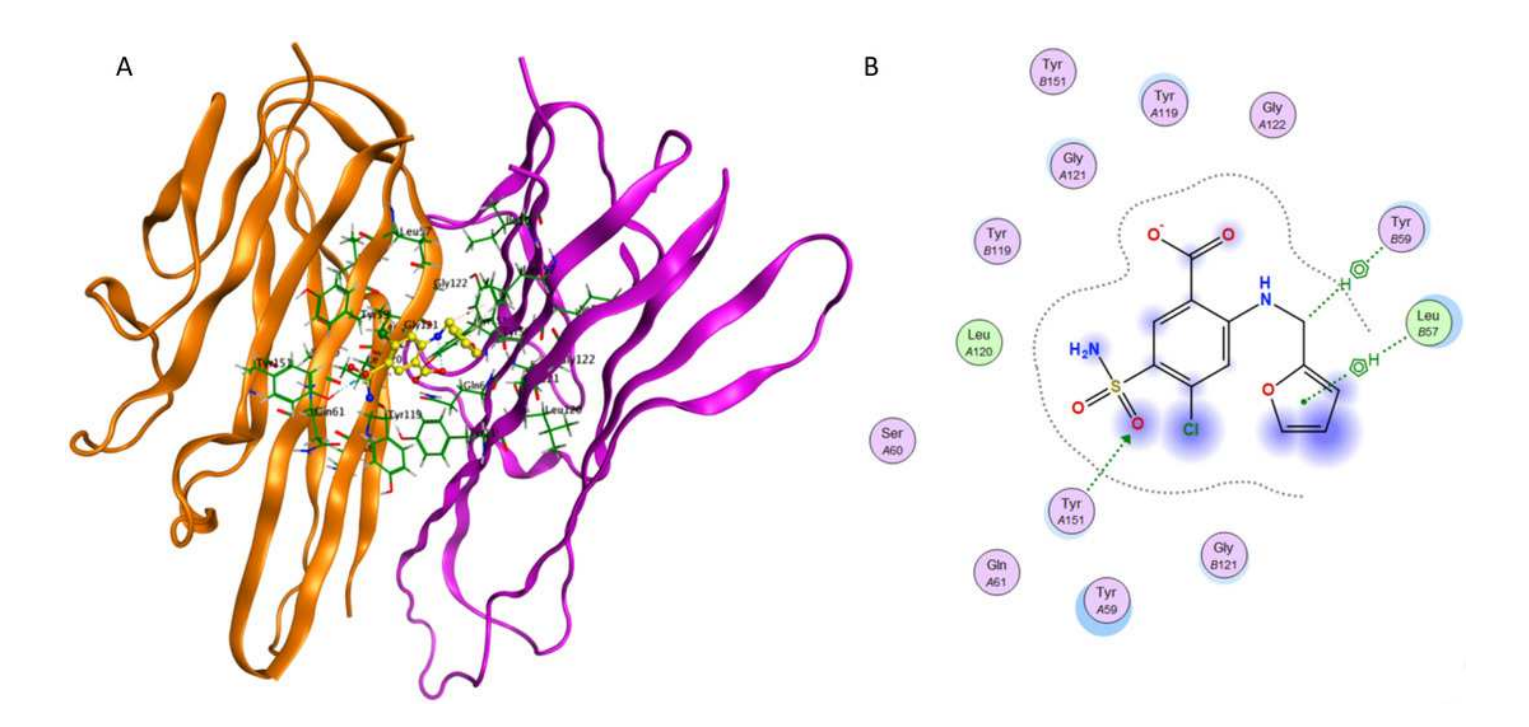
Interaction of 3-HAA with active site of IL-6.

(A) Binding of 3-HAA in the active site of interleukin-6 (IL-6); (B) Ligand interaction diagram of 3-HAA in binding site of IL-6.



Interaction of furosemide with active site of TNF- α .

(A) Binding of furosemide in the active site of tumor necrosis factor α (TNF- α); (B) Ligand interaction diagram of furosemide in binding site of TNF- α .





Interaction of furosemide with active site of IL-6.

Binding of furosemide in the active site of interleukin-6 (IL-6); (B) Ligand interaction diagram of furosemide with binding site of IL-6.

